

***In silico* study of the lipophilicity of the follicular route during topical drug delivery**

Daniel Sebastia-Saez¹, Panayiotis Kattou¹, Guoping Lian^{1,2}, Liang Cui³, Tao Chen^{1*}

¹Department of Chemical and Process Engineering, University of Surrey, Guildford, GU2 7XH, United Kingdom

²Unilever Colworth Science Park, Sharnbrook, Bedfordshire, MK44 1 LQ, United Kingdom

³Department of Civil Engineering, University of Surrey, Guildford, GU2 7XH, United Kingdom

Abstract

Purpose. To study the effect of the lipophilicity of the follicular route on the overall permeation of a given substance into the skin, as *in vitro* and *in vivo* experimental results for skin permeation found in the literature provide inconclusive information on this matter.

Method. We use an *in silico* skin permeation mechanistic model to simulate the dermal delivery of 30 small molecules (molecular weight <500 Da) widely used in pharmacology. The model is complemented with partition and diffusion properties computed from established quantitative structure-property relationships. The simulations are run considering two different scenarios: With the follicular route assumed to be filled with sebum (lipophilic) and filled with water (hydrophilic).

Results. The simulation results show that the relationship between the contribution of the follicular route on the permeation process and the lipophilicity of the compounds follow a linear trend for both scenarios studied. A follicular gap filled with sebum favours the permeation of lipophilic compounds, while the permeation of hydrophilic compounds is favoured with a follicular gap filled with water. The results obtained with the follicular gap filled with water give satisfactory quantitative comparison with *in vitro* experimental data.

Conclusion. The results suggest that the substance filling the follicular gap may undergo alterations prior to *in vitro* testing. Therefore, further experimentation would be interesting to fully elucidate such alterations, which are critical for improving the understanding of the role of the follicular route in skin permeation.

Keywords: in silico modelling; follicular route; dermal absorption; skin permeability; hair follicle

Nomenclature

Latin symbols

c	Concentration	[mol·m ⁻³]
D_{SC}, D_{SE}, D_W	Diffusion coefficient in the stratum corneum, sebum and water, respectively	[m ² ·s ⁻¹]
f_{cat}	Fraction of solute which has been ionised with positive charge	[-]
f_{non}	Fraction of solute which is not ionised	[-]
CHF	Contribution of the follicular route	[-]
\vec{j}	Flux vector	[mol·m ⁻² ·s ⁻¹]
k_B	Boltzmann constant	[J·K ⁻¹]
K_p	Permeability	[cm·s ⁻¹]
$K_{O/W}, K_{SC/W}, K_{SE/W}$	Partition coefficient between octanol and water, between the stratum corneum and water, and between sebum and water, respectively	[-]
MW	Molecular weight	[Da]
r	Solute radius	[Å]
t	Time	[s]
w	Mass fraction of the i th medium	[-]
<u>Greek symbols</u>		
δ	Thickness of the stratum corneum	[μm]

ϕ_i	Volume fraction of the i^{th} medium	[-]
η	Dynamic viscosity	[Pa·s]

Introduction

Understanding the penetration of chemicals through human skin is of high importance to topical drug delivery, personal care, as well as risk assessment of chemical exposure. Many experimental studies have shown that the follicular route contributes significantly to dermal permeation for a wide range of small molecules (generally those with a molecular weight smaller than 500 Da) [1–4]. Experimental studies reported so far on the contribution of the follicular route on the overall permeation of a substance provide, however, inconclusive information on whether the follicular route favours the permeation of hydrophilic or lipophilic compounds. This has significant implications on understanding the delivery and safety of dermatological drugs and skin care actives. Table 1 gathers data on follicular permeation studies published in the last two decades. *In vivo* results suggest that the follicular route favours the permeation of lipophilic compounds. This is expected as, *in vivo*, the sebaceous gland, which together with the hair follicle forms the pilosebaceous unit, secretes sebum continuously into the follicular gap. However, under *in vitro* dermal absorption tests, chemical and physical alterations to the substance filling the follicular gap may occur, modifying the permeation results and hindering their interpretation. For instance, one major alteration is that the continuous secretion of sebum into the follicular gap ceases to occur under *in vitro* conditions. Also, specimens are often soaked in aqueous solutions such as PBS (phosphate buffer solutions) prior to permeation experiments, which together with freezing and thawing of samples stored at low temperatures, can contribute to altering the physico-chemical properties of the substance filling the follicular gap. These alterations could favour the permeation of hydrophilic compounds in a greater extent *in vitro* than *in vivo*.

Table 1 Summary of studies on the effect of the follicular route on overall permeation of small molecules.

Reference	Test condition	Compound(s)	MW [Da]	log $K_{o/w}$	Finding
Otberg et al (2008) [5]	<i>In vivo</i>	Caffeine	194	-0.07	The follicular route significantly increases the concentration in blood plasma ^a .
Teichmann et al. (2005) [6]	<i>In vivo</i>	Sodium Fluorescein (SF)	376	-0.61	SF was recovered from follicular casts after experiment (3% of the dose was in the hair infundibulum, 51% in corneocytes and the remainder was absorbed).
Teichmann et al. (2007)	<i>In vivo</i>	Curcumin	368	3.30	Curcumin permeates into the skin mainly through lipid and follicular route.
Schwartz et al. (2011) [7]	<i>In vivo</i>	Zinc pyrithione (ZP)	317	0.90	Significant amount of ZP detected in follicular gap post-assay.
Ossadnik et al. (2007) [8]	<i>In vivo</i>	Brilliant green solution	482	2.02	Brilliant green solution detected in follicular gap post-assay.
Grams and Bouwstra (2002) [9]	<i>Ex vivo</i>	Bodipy FLc5	320	1.20	Bodipy FLc5 and Bodipy 564/570C5 detected in follicular gap post-assay, but not Oregon Green 488.
		Bodipy 564/570C5	463	3.00	
		Oregon Green 488	509	-2.50	
Chandrasekaran et al. (2016) [10]	<i>In vitro</i>	Magnesium	23	-1.10	Magnesium permeates better into the skin when the hair follicles are not closed.
Genina et al. (2002) [11]	<i>In vivo & in vitro</i>	Dye Indigo Carmine (IG)	466	3.72	Both substances were present in the hair follicle after <i>in vivo</i> assays, but ICG permeates faster <i>in vitro</i> .
		Dye Indocyanine Green (ICG)	775	-0.29	
Frum et al. (2007) [12]	<i>In vitro</i>	Estradiol	272	2.29	The follicular route does not show a clear relationship with the lipophilicity of the compound in this study.
		Corticosterone	346	1.94	
		Hydrocortisone	362	1.60	
		Aldosterone	360	1.08	
		Cimetidine	252	0.40	
		Deoxyadenosine	251	-0.55	
		Adenosine	267	-1.05	
Ogiso et al. (2002) [13]	<i>In vitro</i>	Ketoprofen (KP)	254	3.12	Flux of KP much higher than that observed for MT and 5FU. Histological
		Melatonin (MT)	232	1.18	

		Fluorouracil (5FU)	130	-0.89	observations confirmed permeation had occurred through the follicular gap.
Mohd et al. (2016) [14]	<i>In vitro</i>	Fluorescein isothiocyanate-dextran	4000	-0.77	The follicular pathway clearly favoured the permeation of hydrophilic compounds, with a linear relationship between $\log K_{o/w}$ and contribution of the follicular route.
		Calcein sodium salt	644	-3.50	
		Fluorescein sodium salt	376	-0.61	
		Isosorbide dinitrate	236	1.23	
		Lidocaine hydrochloride	234	-0.9/1.4 ^b	
		Aminopyrine	231	-1/0.98 ^b	
		Ibuprofen	206	1.9/1.3 ^b	
		Butyl paraben	194	3.50	
		Isosorbide mononitrate	191	-0.15	
Essa et al. (2002) [15]	<i>In vitro</i>	Estradiol	272	2.29	Greater contribution of the follicular route for hydrophilic than lipophilic compounds.
		Mannitol	182	-2.47	
		Liposomes			
Tampucci et al. (2014) [16]		Finasteride	373	1.26	Contraction of elastic fibres <i>in vitro</i> postulated as the cause of the underestimation of the recovery of finasteride in the follicular cast <i>in vitro</i> relative to <i>in-vivo</i> .

^aThe contribution of the follicular route on overall absorption was not reported in the experiment; rather, it was determined to be very small by an *in silico* study when the model provided good agreement with the plasma measurement [17]. ^bTwo values were obtained depending on the pH of the buffer solution used.

Of the studies included in Table 1, Mohd et al. [14] and Frum et al. [18] investigated *in vitro*, the contribution of the follicular route on the overall skin permeation for a set of compounds with a significant range of lipophilicity. Mohd et al. [14] tested nine compounds with lipophilicity in the range $\log K_{o/w} \in [-3.5, 3.5]$ and found a significant reduction of the overall skin permeability for hydrophilic compounds upon hair follicle blocking, therefore suggesting that the follicular route favours the permeation of hydrophilic compounds. They also found a linear trend between the contribution of the hair follicle and $\log K_{o/w}$ of the compound. Frum et al. [18] studied the permeation through the follicular route of seven compounds with lipophilicity $\log K_{o/w} \in [-1.05, 2.29]$. For the two most lipophilic compounds tested, the effect of the follicular route was very small, which would indicate that the hair follicle acts as a

hydrophilic route. For the rest of the compounds tested, however, the authors suggest that not the lipophilicity, but other molecular properties, play a more important role on the contribution of the follicular route on dermal permeation. Finally, an *ex vivo* experiment, arguably more closely mimicking the *in vivo* conditions than an *in vitro* test, by Grams and Bouwstra [9] designated the hair follicle as a lipophilic route.

In this work, we used our recently reported two-dimensional, mechanistic skin permeation model [19–23] to investigate the contribution of the follicular route on the permeation process. The model is used in conjunction with state-of-the-art quantitative structure-property relationships (QSPR) reported in the literature to quantify partition and diffusion coefficients needed to run the skin permeation model. The results show good agreement with *in vitro* experimental data when the follicular route is modelled as being hydrophilic, hence confirming that alterations in the composition of the substance filling the follicular gap do occur prior to *in vitro* dermal permeation tests. These alterations are worth being studied in order to better comprehend the role of the follicular route in dermal permeation.

Methodology

The commercial Finite-Element-Method modelling package COMSOL Multiphysics 5.5 was employed to implement the *in silico* skin permeation model. The geometry of the simulation set-up is depicted in Fig. 1. It consists of three subdomains, which represent the stratum corneum, follicular gap and the hair shaft. A two-dimensional domain was necessary in order to describe the lateral flux in the vicinity of the follicular gap. The vehicle has been represented in the schematic for clarity and has been simulated as a boundary condition of fixed concentration (infinite dose). The partition coefficients between the vehicle and the stratum corneum ($K_{vh/sc}$), and between the vehicle and the follicular gap ($K_{vh/fp}$), with the vehicle set as an aqueous medium, are taken into account to establish the boundary conditions. A zero concentration is imposed on the bottom boundary of the domain, representing a sink condition.

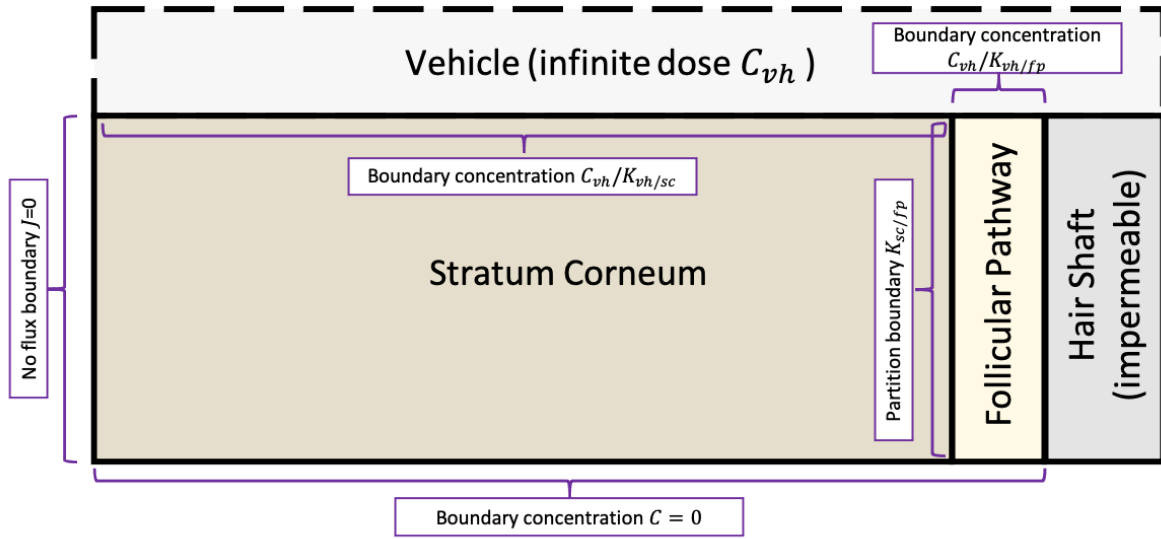


Fig. 1 Schematic illustration of the computational domain. Not to scale.

The schematic illustration in Fig. 1 is not to scale. The fraction of the skin area occupied by hair follicles vary across the position in human body. Some representative values are gathered in Table 2. The value used here is the average (0.38%), with the radius of the hair being $35 \mu\text{m}$, and the radius of the hair orifice $48 \mu\text{m}$. To keep the area ratio (0.38%), the horizontal dimensions of the simulation domain are $119.6 \mu\text{m}$ for the stratum corneum and $0.17 \mu\text{m}$ for the follicular pathway. The vertical dimension (thickness) is $14.1 \mu\text{m}$ [24].

Table 2 Dimensions of the hair follicle depending on body site [25–30].

Site	Stratum corneum thickness [μm]	Hair radius [μm]	Area of follicular orifice over entire body skin area [%]	Hair orifice radius [μm]
Chest	14.80	40	0.19	50
Forearm	12.98	32	0.09	40
Abdomen	14.52	40	0.19	50
Scalp	14.36	15	1.28	30

Back	14.39	40	0.33	52
Thigh	12.28	55	0.23	65

The diffusion equation with no convection was solved:

$$\frac{\partial c}{\partial t} + \nabla \cdot \vec{J} = 0, \quad (1)$$

where c represents the concentration, t is the time and the diffusion flux is $\vec{J} = -D\nabla c$ (with D being the diffusion coefficient).

The diffusion and partition parameters were calculated and subsequently input to the simulation set-up. The overall properties of the stratum corneum were considered instead of the ‘bricks-and-mortar’ structure [31] as this work is focused on the contribution of the hair follicle. The following expression gives the partition coefficient, as a concentration ratio, between the homogenised stratum corneum and water [32]:

$$K_{sc/w} = \left(\phi_{pro} \times \frac{\rho_{pro}}{\rho_w} \times K_{pro/w} + \phi_{lip} \times \frac{\rho_{lip}}{\rho_w} \times K_{lip/w} + \phi_w \right) \times \frac{\rho_w}{\rho_{sc}}, \quad (2)$$

where ϕ is the volume fraction. The subindices *pro*, *lip*, *w* and *sc* denote protein, lipid, water and stratum corneum respectively. The partition coefficient of protein to water $K_{pro/w}$ is obtained by means of the following QSPR:

$$K_{pro/w} = 4.23 \times (K_{o/w})^{0.31}, \quad (3)$$

and the QSPR for the partition of lipid to water is

$$K_{lip/w} = (K_{o/w})^{0.69}. \quad (4)$$

Both $K_{pro/w}$ and $K_{lip/w}$ were obtained by Wang et al. [33] over an experimental data set with a correlation coefficient $R^2 = 0.89$ (logarithmic scale).

The volume fractions ϕ of protein, lipid and water in the stratum corneum are obtained considering the mass fractions of protein and lipid in dry stratum corneum ($w_{pro/dry_sc}=0.77$ and $w_{lip/dry_sc}=0.23$), the mass of water absorbed per unit mass of dry stratum corneum ($v=2.99$), and the densities of the three components ($\rho_{pro}=1.37 \text{ g}\cdot\text{cm}^{-3}$, $\rho_{lip}=0.9 \text{ g}\cdot\text{cm}^{-3}$ and $\rho_w=1 \text{ g}\cdot\text{cm}^{-3}$) as measured by Wang et al. [32].

The diffusion coefficient of the homogenised stratum corneum D_{sc} is calculated by its relationship with the permeability of the stratum corneum K_p :

$$D_{sc} = \frac{K_p \delta}{K_{sc/w}}, \quad (5)$$

where $K_{sc/w}$ is the partition coefficient between the stratum corneum and water, and δ is the thickness of the stratum corneum. Experimental values of the permeability obtained by Johnson et al. for a thickness of the stratum corneum $\delta = 14.1 \mu\text{m}$ were input to Eqn 5 to obtain the diffusion coefficients [24].

The following QSPR ($R^2=0.92$, logarithmic scale) was developed specifically to calculate the diffusion in sebum [34]:

$$D_{se} [m^2/s] = 2.48 \times 10^{-4} e^{-0.42r^2}, \quad (6)$$

where the solute radius is calculated as $r [\text{\AA}] = \sqrt[3]{\frac{3}{4\pi} \times 0.9087MW}$. The partition coefficients of solutes between sebum and water were calculated using the QSPR reported by Yang et al. [35], which considers the degree of ionisation of the compound and has proved to give better results ($R^2=0.89$) than previous QSPRs models available in the literature:

$$\log K_{se/w} = \log \left\{ f_{non} \left(\frac{1+0.71 \times 10^{pH-6.95}}{1+10^{pH-6.95}} \right) + f_{cat} \frac{1.23 \times 10^{pH-6.95}}{1+10^{pH-6.95}} \right\} + 0.79 \log K_{o/w}, \quad (7)$$

where f_{non} is the fraction of the component that remains non-ionised and f_{cat} is the fraction of the component which is ionised and has positive charge. Both fractions are obtained from the <http://ilaboffsite.psds.ac.uk/> database. For skin, $pH=5.7$ has been considered [36].

The diffusion coefficients in water were obtained by means of the Stokes-Einstein equation:

$$D_w = \frac{k_B T}{6\pi\eta r}, \quad (8)$$

where k_B is the Boltzmann constant, T is the temperature, η is the dynamic viscosity and r is the solute radius.

The contribution of the follicular route CFR , is calculated as a percentage of the increased skin permeability with the hair follicle open to closed, as follows:

$$CFR [\%] = \frac{|\log K_{p_open} - \log K_{p_closed}|}{|\log K_{p_open}|} \times 100, \quad (9)$$

where $K_{p_open} = J/C_{vh}$.

Table 3 shows the input data to the QSPRs for the 30 compounds included in this *in silico* study. These 30 compounds present a sufficiently broad range of octanol-water partition coefficients $\log K_{o/w} \in [-3.70, 4.05]$, molecular weight $MW \in [32, 585] Da$, and non-ionised fraction f_{non} to cover the values usually found in topical drug delivery of small molecules.

Table 3 List of input parameters to calculate diffusion and partition coefficients.

Substance	f_{non}	f_{cat}	MW [Da]	Solute radius [Å]	log Ko/w	log Kp ^a [cm/s]
Estradiol	1.00	0.00	272.00	3.89	4.01	-5.84
Hydrocortisone	1.00	0.00	362.00	4.28	1.61	-7.48
Piroxicam	0.39	0.61	331.00	4.16	3.06	-7.37
Sucrose	1.00	0.00	342.00	4.20	-3.70	-8.84
Scopolamine	0.01	0.99	303.00	4.04	0.98	-7.86

Phenobarbital	0.98	0.00	232.00	3.69	1.47	-6.89
Nitroglycerine	1.00	0.00	227.00	3.67	1.62	-5.51
Naproxen	0.04	0.00	230.00	3.68	3.18	-6.95
Morphine	0.00	1.00	285.00	3.95	0.89	-8.59
Meperidine	0.00	1.00	247.00	3.77	2.72	-5.99
Fentanyl	0.00	1.00	336.00	4.18	4.05	-5.81
Codeine	0.00	1.00	299.00	4.02	4.05	-5.81
Aniline	0.93	0.07	93.00	2.72	0.90	-5.21
Barbital	0.99	0.00	184.00	3.42	0.65	-7.51
Benzaldehyde	1.00	0.00	106.00	2.84	1.48	-4.41
Benzene	1.00	0.00	78.00	2.57	2.13	-4.51
Benzyl Alcohol	1.00	0.00	108.00	2.86	1.10	-5.33
Butanol	1.00	0.00	74.00	2.52	0.88	-6.16
Butobarbital	0.99	0.00	212.00	3.58	1.73	-7.27
Chlorpheniramine	0.00	1.00	275.00	3.91	3.38	-6.22
Decanol	1.00	0.00	158.00	3.25	4.57	-4.65
Diethylcarbazine	0.07	0.93	199.00	3.51	0.37	-7.45
Dyhydromorphine	0.00	1.00	287.00	3.96	0.93	-8.38
Ephedrine	0.00	1.00	165.00	3.30	1.13	-5.78
Ethanol	1.00	0.00	46.00	2.15	-0.31	-6.65
Methanol	1.00	0.00	32.00	1.91	-0.77	-6.86
Ouabain	1.00	0.00	585.00	5.03	-2.00	-9.66
p-Phenylenediamine	0.24	0.76	108.00	2.86	-0.30	-7.18
Urea	1.00	0.00	61.00	2.37	-2.11	-7.39
n-Nitrosodiethanolamine	1.00	0.00	134.00	3.07	-1.28	-8.30

^aExperimental *in vitro* values of the permeability from Johnson et al. [24] were used to obtain the diffusion coefficient of a given substance through the stratum corneum (Eqn 5).

Results and discussion

Table 4 Input variables to the skin permeation model: Partition and diffusion coefficients

Substance	$K_{se/w}$	$K_{sc/w}$	$D_w \times 10^{-10}$ [m ² /s]	$D_{se} \times 10^{-11}$ [m ² /s]	$D_{sc} \times 10^{-15}$ [m ² /s]
Estradiol	1449.25	48.63	6.20	1.02	4.46
Hydrocortisone	18.41	4.06	5.63	0.28	1.22
Piroxicam	110.84	15.42	5.80	0.44	0.42
Sucrose	0.00	0.81	5.74	0.37	0.27
Scopolamine	0.44	2.66	5.98	0.65	0.78
Phenobarbital	13.99	3.67	6.53	1.80	5.27
Nitroglycerine	18.75	4.09	6.58	1.93	113
Naproxen	12.81	17.63	6.55	1.85	0.96

Morphine	0.33	2.52	6.10	0.84	0.15
Meperidine	9.22	10.76	6.40	1.45	14.3
Fentanyl	103.67	51.25	5.78	0.41	4.53
Codeine	103.67	51.25	6.00	0.69	4.53
Aniline	4.73	2.54	8.86	13.1	365
Barbital	3.18	2.21	7.06	3.57	2.10
Benzaldehyde	14.54	3.69	8.48	10.9	1580
Benzene	47.42	6.17	9.40	16.2	751
Benzyl Alcohol	7.28	2.86	8.43	10.6	245
Butanol	4.88	2.51	9.56	17.2	41.4
Butobarbital	22.68	4.45	6.73	2.39	1.81
Chlorpheniramine	30.64	22.201	6.17	0.97	4.07
Decanol	4013.68	103.87	7.43	5.17	32.3
Diethylcarbazine	0.25	1.91	6.88	2.88	2.78
Dyhydromorphine	0.36	2.58	6.09	0.82	0.26
Ephedrine	0.51	2.92	7.32	4.68	85.3
Ethanol	0.56	1.44	11.2	25.6	23.4
Methanol	0.24	1.24	12.6	31.3	16.8
Ouabain	0.03	0.95	4.80	0.01	0.03
p-Phenylenediamine	0.17	1.44	8.43	10.6	6.88
Urea	0.02	0.93	10.2	20.7	6.57
n-Nitrosodiethanolamine	0.10	1.08	7.85	7.29	0.70

The diffusion and partition coefficients of the 30 compounds obtained by using the QSPRs included in the methodology section are listed in Table 4. These were input to the model set-up to obtain the time evolution of the concentration within the stratum corneum and the follicular gap for 50 hours diffusion time, after which, the percentage of change with respect to the previous time step was below 0.01% in all of the cases, hence confirming that steady state conditions were reached. The spatial distribution of the concentration within the model geometry at steady state was used to derive the permeability, and then, the contribution of the follicular route in the permeation process (Eqn 9). The data were fitted to a linear trend with correlation coefficient $R^2=0.52$ (sebum tube) and $R^2=0.43$ (water tube). The linear fitting is intended only as a visual aid to highlight the trend followed by the model data, thus facilitating the analysis by comparison with the experimental data available in the literature [14,18] (Fig. 2). The model data for a water tube are of similar trend and magnitude to those reported by

Frum et al. [18] and Mohd et al. [14]. The opposite is observed when the follicular route is assumed to be filled with sebum. This comparison confirms, therefore, that *in vitro*, the follicular route behaves as a hydrophilic medium. Therefore, in order to be consistent with these observations, the follicular pathway must undergo changes prior to *in vitro* experimentation.

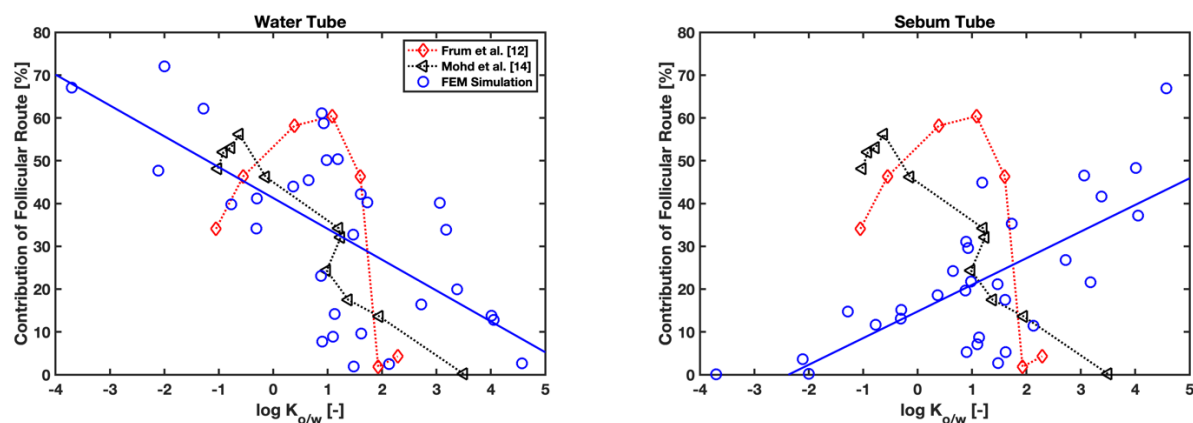


Fig. 2 Comparison between skin permeation model and available experimental data.

Conclusions

In this work, a previously developed skin permeation model, combined with state-of-the-art quantitative structure-property relationships, has been used to advance the understanding of the contribution of the follicular route on dermal permeation. To this end, the permeation of 30 compounds was simulated twice: One assuming the follicular gap as being a hydrophilic route (a water tube), and another assuming it as being a lipophilic route (a sebum tube). The 30 compounds were chosen to encompass the range of lipophilicity and molecular weights often found in real scenarios of dermal permeation for small molecules (< 30 Da).

Linear trends were found upon both assumptions (water and sebum follicular gap) for the relationship between the contribution of the hair follicle and the lipophilicity of the compound being tested. In the case of the follicular gap being filled with sebum, the contribution of the follicular route increases with the lipophilicity of the compound. When the follicular gap is

assumed to be filled with water, however, the contribution of the follicular route decreases with the lipophilicity of the compound. Moreover, the simulation data obtained by assuming the follicular route as a hydrophilic route (filled with water) match in trend and order of magnitude the available experimental data *in vitro*.

The results confirm, thus, the occurrence of changes in the composition of the follicular route between excision from a living donor and experimentation *in vitro*. It would be advisable, therefore, to analyse the alterations occurring in that interim, in order to be able to interpret results *in vitro* confidently.

Acknowledgements

The authors would like to gratefully acknowledge the financial support from the UK Engineering and Physical Science Research Council (EPSRC), project: EP/S021167/1.

References

1. Otberg N, Patzelt A, Rasulev U, Hagemeister T, Linscheid M, Sinkgraven R, et al. The role of hair follicles in the percutaneous absorption of caffeine. *Br J Clin Pharmacol*. 2008;65:488–92.
2. Prausnitz MR, Mitragotri S, Langer R. Current status and future potential of transdermal drug delivery. *Nat Rev Drug Discov*. 2004;3:115–24.
3. Alkilani AZ, McCrudden MTC, Donnelly RF. Transdermal drug delivery: Innovative pharmaceutical developments based on disruption of the barrier properties of the stratum corneum. *Pharmaceutics*. 2015;7:438–70.
4. Leite-Silva VR, De Almeida MM, Fradin A, Grice JE, Roberts MS. Delivery of drugs applied topically to the skin. *Expert Rev Dermatol*. 2012;7:383–97.
5. Otberg N, Patzelt A, Rasulev U, Hagemeister T, Linscheid M, Sinkgraven R, et al. The role of hair follicles in the percutaneous absorption of caffeine. *Br J Clin Pharmacol*. 2008;65:488–92.
6. Teichmann A, Jacobi U, Ossadnik M, Richter H, Koch S, Sterry W, et al. Differential Stripping: Determination of the Amount of Topically Applied Substances Penetrated into the Hair Follicles. *J Invest Dermatol*. 2005;125:264–9.
7. Schwartz JR, Shah R, Krigbaum H, Sacha J, Vogt A, Blume-Peytavi U. New insights on dandruff/seborrheic dermatitis: The role of the scalp follicular infundibulum in effective treatment strategies. *Br J Dermatol*. 2011;165:18–23.
8. Ossadnik M, Czaika V, Teichmann A, Sterry W, Tietz H-J, Lademann J, et al. Differential stripping: introduction of a method to show the penetration of topically applied antifungal substances into the hair follicles. *Mycoses*. 2007;50:457–62.
9. Grams, Bouwstra JA. Penetration and distribution of three lipophilic probes in vitro in human skin focusing on the hair follicle. *J Control Release*. 2002;83:253–62.

10. Chandrasekaran NC, Sanchez WY, Mohammed YH, Grice JE, Roberts MS, Barnard RT. Permeation of topically applied Magnesium ions through human skin is facilitated by hair follicles. *Magnes Res.* 2016;29:35–42.
11. Genina E a, Bashkatov AN, Sinichkin YP, Kochubey VI, Lakodina N a, Altshuler GB, et al. In vitro and in vivo study of dye diffusion into the human skin and hair follicles. *J Biomed Opt.* 2002;7:471–7.
12. Frum Y, Bonner MC, Eccleston GM, Meidan VM. The influence of drug partition coefficient on follicular penetration: In vitro human skin studies. *Eur J Pharm Sci.* 2007;30:280–7.
13. Ogiso T, Shiraki T, Okajima K, Tanino T, Iwaki M, Wada T. Transfollicular drug delivery: penetration of drugs through human scalp skin and comparison of penetration between scalp and abdominal skins in vitro. *J Drug Target.* 2002;10:369–78.
14. Mohd F, Todo H, Yoshimoto M, Yusuf E, Sugibayashi K. Contribution of the Hair Follicular Pathway to Total Skin Permeation of Topically Applied and Exposed Chemicals. *Pharmaceutics.* 2016;8:32.
15. Essa EA, Bonner MC, Barry BW. Human skin sandwich for assessing shunt route penetration during passive and iontophoretic drug and liposome delivery. *J Pharm Pharmacol.* 2002;54:1481–90.
16. Tampucci S, Burgalassi S, Chetoni P, Lenzi C, Pirone A, Mailland F, et al. Topical formulations containing finasteride. part II: Determination of finasteride penetration into hair follicles using the differential stripping technique. *J Pharm Sci.* 2014;103:2323–9.
17. Kattou P. Mathematical modelling of transdermal permeation of chemicals with special focus on the hair follicle pathway. PhD thesis. University of Surrey; 2017.
18. Frum Y, Bonner MC, Eccleston GM, Meidan VM. The influence of drug partition coefficient on follicular penetration: in vitro human skin studies. *Eur J Pharm Sci.*

2007;30:280–7.

19. Kattou P, Lian G, Glavin S, Sorrell I, Chen T. Development of a Two-Dimensional Model for Predicting Transdermal Permeation with the Follicular Pathway: Demonstration with a Caffeine Study. *Pharm Res. Pharmaceutical Research*; 2017;34:2036–48.

20. Coleman L, Lian G, Glavin S, Sorrell I, Chen T. In Silico Simulation of Simultaneous Percutaneous Absorption and Xenobiotic Metabolism: Model Development and a Case Study on Aromatic Amines. *Pharm Res. Pharmaceutical Research*; 2020;37:1–10.

21. Chen T, Lian G, Kattou P. In Silico Modelling of Transdermal and Systemic Kinetics of Topically Applied Solutes: Model Development and Initial Validation for Transdermal Nicotine. *Pharm Res [Internet]. Pharmaceutical Research*; 2016;33:1602–14. Available from: <http://dx.doi.org/10.1007/s11095-016-1900-x>

22. Chen L, Lian G, Han L. Use of “bricks and mortar” model to predict transdermal permeation: Model development and initial validation. *Ind Eng Chem Res.* 2008;47:6465–72.

23. Sebastia-Saez D, Burbidge A, Engmann J, Ramaioli M. New trends in mechanistic transdermal drug delivery modelling: Towards an accurate geometric description of the skin microstructure. *Comput Chem Eng [Internet]. Elsevier Ltd*; 2020;141:106976. Available from: <https://doi.org/10.1016/j.compchemeng.2020.106976>

24. Johnson ME, Blankschtein D, Langer R. Evaluation of solute permeation through the stratum corneum: lateral bilayer diffusion as the primary transport mechanism. *J Pharm Sci.* 1997;86:1162–72.

25. Aboagye B, Ahenkorah J, Hottor B, Addai F. Comparative Characteristics Of Black And Grey Chest And Selected Facial Hairs In Negroid Males. *Internet J Biol Anthropol.* 2014;7:1–14.

26. Lee Y, Hwang K. L'épaisseur de la peau des Coréens adultes. *Surg Radiol Anat.* 2002;24:183–9.

27. Otberg N, Richter H, Schaefer H, Blume-Peytavi U, Sterry W, Lademann J. Variations of Hair Follicle Size and Distribution in Different Body Sites. *J Invest Dermatol*. 2004;122:14–9.
28. Grams YY, Bouwstra JA. Penetration and distribution of three lipophilic probes in vitro in human skin focusing on the hair follicle. *J Control Release*. 2002;83:253–62.
29. Sandby-Møller J, Poulsen T, Wulf HC. Epidermal Thickness at Different Body Sites: Relationship to Age, Gender, Pigmentation, Blood Content, Skin Type and Smoking Habits. *Acta Derm Venereol*. 2003;83:410–3.
30. Tsugita T, Nishijima T, Kitahara T, Takema Y. Positional differences and aging changes in Japanese woman epidermal thickness and corneous thickness determined by OCT (optical coherence tomography). *Ski Res Technol*. 2013;19:242–50.
31. Michaels AS, Chandrasekaran SK, Shaw JE. Drug permeation through human skin: Theory and invitro experimental measurement. *AIChE J*. 1975;21:985–96.
32. Wang L, Chen L, Lian G, Han L. Determination of partition and binding properties of solutes to stratum corneum. *Int J Pharm* [Internet]. Elsevier B.V.; 2010;398:114–22. Available from: <http://dx.doi.org/10.1016/j.ijpharm.2010.07.035>
33. Wang Y, Li K, Gan S, Cameron C. Analysis of energy saving potentials in intelligent manufacturing: A case study of bakery plants. *Energy*. 2019;172:477–86.
34. Yang S, Li L, Lu M, Chen T, Han L, Lian G. Determination of Solute Diffusion Properties in Artificial Sebum. *J Pharm Sci* [Internet]. Elsevier Ltd; 2019;108:3003–10. Available from: <https://doi.org/10.1016/j.xphs.2019.04.027>
35. Yang S, Li L, Chen T, Han L, Lian G. Determining the Effect of pH on the Partitioning of Neutral, Cationic and Anionic Chemicals to Artificial Sebum: New Physicochemical Insight and QSPR Model. *Pharm Res. Pharmaceutical Research*; 2018;35.
36. Ali SM, Yosipovitch G. Skin pH : From Basic Science to Basic Skin Care. 2013;261–7.